articles

molecular pharmaceutics

Vitamin E TPGS P-Glycoprotein Inhibition Mechanism: Influence on Conformational Flexibility, Intracellular ATP Levels, and Role of Time and Site of Access

Eva-Maria Collnot,*,† Christiane Baldes,† Ulrich F. Schaefer,† Kevin J. Edgar,‡,§ Michael F. Wempe,‡,|| and Claus-Michael Lehr†

Biopharmaceutics and Pharmaceutical Technology, Saarland University, 66123 Saarbrücken, Germany, Eastman Chemical Company, Kingsport, Tennessee, Virginia Tech, 230 Cheatham Hall, Blacksburg, Virginia, and Department of Pharmaceutical Sciences, University of Colorado Denver, Aurora, Colorado

Received August 5, 2009; Revised Manuscript Received January 14, 2010; Accepted March 5, 2010

Abstract: Previous work conducted in our laboratories established the notion that TPGS 1000 (D-α-tocopheryl polyethylene glycol 1000 succinate), a nonionic surfactant, modulates P-glycoprotein (P-gp) efflux transport via P-gp ATPase inhibition. The current *in vitro* research using Caco-2 cells was conducted to further explore the P-gp ATPase inhibition mechanism. Using a monoclonal CD243 P-gp antibody shift assay (UIC2), we probed P-gp conformational changes induced via TPGS 1000. In the presence of TPGS 1000, UIC2 binding was slightly decreased. TPGS 1000 does not appear to be a P-gp substrate, nor does it function as a competitive inhibitor in P-gp substrate efflux transport. The reduction in UIC2 binding with TPGS 1000 was markedly weaker than with orthovanadate, data ruling out trapping P-gp in a transition state by direct interaction with one or both of the P-gp ATP nucleotide binding domains. An intracellular ATP depletion mechanism could be ruled out in the UIC2 assay, and by monitoring intracellular ATP levels in the presence of TPGS 1000. Indicating slow distribution of TPGS 1000 into the membrane, and in agreement with an intramembranal or intracellular side of action, Caco-2 cell monolayer experiments preincubated with TPGS 1000 produce stronger substrate inhibitory activity than those conducted by direct substrate and surfactant coapplication.

Keywords: P-glycoprotein; vitamin E TPGS; efflux transporter; inhibition; ATP; conformation

1. Introduction

Drug oral bioavailability may be influenced by intrinsic solubility or instability, low membrane permeability, high first pass metabolism, or active excretion (i.e., efflux pumps) from the enterocytes back into the intestinal lumen. An extensively studied ATP-binding cassette (ABC) superfamily member, and the product of the multi drug resistance gene MDR1, P-glycoprotein (P-gp) predominantly locates in epithelia apical membranes (e.g., luminal surface of small intestine, colon, brain capillary endothelial cells and kidney proximal tubules).[1−7] P-gp protects cells by actively trans-

* Corresponding author. Mailing address: Biopharmaceutics and Pharmaceutical Technology, Saarland University, Campus A4.1, 66123 Saarbruecken, Germany. Phone: +49 681 3022939. Fax: +49 681 3024677. E-mail: e.collnot@mx.uni-saarland.de.

† Saarland University.

‡ Eastman Chemical Company.

§ Virginia Tech.

|| University of Colorado Denver.

(1) Ueda, K.; Cornwell, M. M.; Gottesman, M. M.; Pastan, I.; Roninson, I. B.; Ling, V.; Riordan, J. R. The mdr1 gene, responsible for multidrug-resistance, codes for P-glycoprotein. *Biochem. Biophys. Res. Commun.* **1986**, *141* (3), 956–962.

(2) Higgins, C. F. ABC transporters: from microorganisms to man. *Annu. Rev. Cell Biol.* **1992**, *8*, 67–113.

(3) Thiebaut, F.; Tsuruo, T.; Hamada, H.; Gottesman, M. M.; Pastan, I.; Willingham, M. C. Cellular Localization of the Multidrug-Resistance Gene Product P-glycoprotein in Normal Human Tissues. *Proc. Natl. Acad. Sci. U.S.A.* **1987**, *84* (21), 7735–7738.

(4) Fromm, M. F. Importance of P-glycoprotein at blood-tissue barriers. *Trends Pharmacol. Sci.* **2004**, *25* (8), 423–429.

10.1021/mp900191s
Published on Web 03/05/2010

porting substrates against a concentration gradient and thereby reducing intracellular levels below effective and/or toxic concentration.[8] Located at the enterocyte apical membrane with broad substrate specificity, P-gp may significantly limit drug oral absorption.[9] To enhance substrate oral bioavailability, P-gp may be inhibited by coadministration with compounds such as GF120918 or PSC-833,[10,11] flavonoids,[12] bile salts,[13] or surfactants.[14−20]

A water-soluble form of vitamin E, TPGS 1000 (D-α-tocopheryl polyethylene glycol 1000 succinate) contains a hydrophilic polar (water-soluble) PEG chain and a lipophilic (water-insoluble) α-tocopherol head. TPGS 1000 has been shown to be one of the most potent commercially available P-gp inhibitor surfactants.[20] Due to surface active properties, TPGS 1000 may be used as a drug solubilizer, as an emulsifier, and as a vehicle in lipid based drug delivery formulations. Previously, we disclosed a TPGS structure−activity relationship (SAR) study.[16] We showed that Rhodamine 123 (RHO) efflux inhibition in Caco-2 monolayer transport experiments varied with TPGS PEG chain length (between 200 and 6000 Da); the results afforded a predicted optimal *in vitro* efflux inhibitory effect at a PEG chain length residing between 1581 ± 209 Da (absorptive) and 1182 ± 476 Da (secretory). Besides the analogues with modified PEG chains, a second group of derivatives was introduced which varied in the hydrophobic moiety. Among these analogues, cholesterol PEG 1000 succinate (CPGS) showed the strongest P-gp modulation and surpassed TPGS 1000.[21] In addition, we investigated the mechanism of P-gp inhibition by TPGS 1000.[21] Rigidification or fluidization of the P-gp membrane environment produced by TPGS 1000 at P-gp active concentrations was ruled out as the main cause for inhibition. Instead, P-gp ATPase—the P-gp energy source driving active transport—inhibition was identified as an integral step. However, it remained unclear if P-gp ATPase inhibition was achieved (i) via a direct interaction of TPGS 1000 with the P-gp nucleotide binding domains (NBD); (ii) indirectly via an allosteric modulation of the P-gp function; or (iii) via steric blocking of substrate binding. P-gp ATPase inhibition has been previously demonstrated for another group of P-gp active nonionic surfactants.[22,23] Batrakova et al. have attributed the P-gp inhibitory effect of several Pluronic block

(5) Mizuno, N.; Niwa, T.; Yotsumoto, Y.; Sugiyama, Y. Impact of drug transporter studies on drug discovery and development. *Pharmacol. Rev.* **2003**, *55* (3), 425–461.
(6) Lankas, G. R.; Wise, L. D.; Cartwright, M. E.; Pippert, T.; Umbenhauer, D. R. Placental P-glycoprotein deficiency enhances susceptibility to chemically induced birth defects in mice. *Reprod. Toxicol.* **1998**, *12* (4), 457–463.
(7) van der Valk, P.; van Kalken, C. K.; Ketelaars, H.; Broxterman, H. J.; Scheffer, G.; Kuiper, C. M.; Tsuruo, T.; Lankelma, J.; Meijer, C. J.; Pinedo, H. M. Distribution of multi-drug resistance-associated P-glycoprotein in normal and neoplastic human tissues. Analysis with 3 monoclonal antibodies recognizing different epitopes of the P-glycoprotein molecule. *Ann. Oncol.* **1990**, *1* (1), 56–64.
(8) Roninson, I. B. Molecular mechanism of multidrug resistance in tumor cells. *Clin. Physiol. Biochem.* **1987**, *5* (3−4), 140–151.
(9) Suzuki, H.; Sugiyama, Y. Role of metabolic enzymes and efflux transporters in the absorption of drugs from the small intestine. *Eur. J. Pharm. Sci.* **2000**, *12* (1), 3–12.
(10) Malingre, M. M.; Beijnen, J. H.; Rosing, H.; Koopman, F. J.; Jewell, R. C.; Paul, E. M.; Ten Bokkel Huinink, W. W.; Schellens, J. H. Co-administration of GF120918 significantly increases the systemic exposure to oral paclitaxel in cancer patients. *Br. J. Cancer* **2001**, *84* (1), 42–47.
(11) Cagliero, E.; Ferracini, R.; Morello, E.; Scotlandi, K.; Manara, M. C.; Buracco, P.; Comandone, A.; Baroetto Parisi, R.; Baldini, N. Reversal of multidrug-resistance using Valspodar (PSC 833) and doxorubicin in osteosarcoma. *Oncol. Rep.* **2004**, *12* (5), 1023–1031.
(12) Kitagawa, S.; Nabekura, T.; Takahashi, T.; Nakamura, Y.; Sakamoto, H.; Tano, H.; Hirai, M.; Tsukahara, G. Structure-activity relationships of the inhibitory effects of flavonoids on P-glycoprotein-mediated transport in KB-C2 cells. *Biol. Pharm. Bull.* **2005**, *28* (12), 2274–2278.
(13) Schuldes, H.; Dolderer, J. H.; Zimmer, G.; Knobloch, J.; Bickeboller, R.; Jonas, D.; Woodcock, B. G. Reversal of multidrug resistance and increase in plasma membrane fluidity in CHO cells with R-verapamil and bile salts. *Eur. J. Cancer* **2001**, *37* (5), 660–667.
(14) Dintaman, J. M.; Silverman, J. A. Inhibition of P-glycoprotein by D-alpha-tocopheryl polyethylene glycol 1000 succinate (TPGS). *Pharm. Res.* **1999**, *16* (10), 1550–1556.
(15) Shono, Y.; Nishihara, H.; Matsuda, Y.; Furukawa, S.; Okada, N.; Fujita, T.; Yamamoto, A. Modulation of intestinal P-glycoprotein function by cremophor EL and other surfactants by an in vitro diffusion chamber method using the isolated rat intestinal membranes. *J. Pharm. Sci.* **2004**, *93* (4), 877–885.
(16) Collnot, E. M.; Baldes, C.; Wempe, M. F.; Hyatt, J.; Navarro, L.; Edgar, K. J.; Schaefer, U. F.; Lehr, C. M. Influence of vitamin E TPGS poly(ethylene glycol) chain length on apical efflux transporters in Caco-2 cell monolayers. *J. Controlled Release* **2006**, *111* (1−2), 35–40.
(17) Bogman, K.; Erne-Brand, F.; Alsenz, J.; Drewe, J. The role of surfactants in the reversal of active transport mediated by multidrug resistance proteins. *J. Pharm. Sci.* **2003**, *92* (6), 1250–1261.
(18) Cornaire, G.; Woodley, J.; Hermann, P.; Cloarec, A.; Arellano, C.; Houin, G. Impact of excipients on the absorption of P-glycoprotein substrates in vitro and in vivo. *Int. J. Pharm.* **2004**, *278* (1), 119–131.
(19) Johnson, B. M.; Charman, W. N.; Porter, C. J. An in vitro examination of the impact of polyethylene glycol 400, Pluronic P85, and vitamin E d-alpha-tocopheryl polyethylene glycol 1000 succinate on P-glycoprotein efflux and enterocyte-based metabolism in excised rat intestine. *AAPS PharmSci* **2002**, *4* (4), E40.
(20) Rege, B. D.; Kao, J. P.; Polli, J. E. Effects of nonionic surfactants on membrane transporters in Caco-2 cell monolayers. *Eur. J. Pharm. Sci.* **2002**, *16* (4−5), 237–246.
(21) Collnot, E. M.; Baldes, C.; Wempe, M. F.; Kappl, R.; Huttermann, J.; Hyatt, J. A.; Edgar, K. J.; Schaefer, U. F.; Lehr, C. M. Mechanism of Inhibition of P-Glycoprotein Mediated Efflux by Vitamin E TPGS: Influence on ATPase Activity and Membrane Fluidity. *Mol. Pharmaceutics* **2007**, *4* (3), 465–474.
(22) Orlowski, S.; Selosse, M. A.; Boudon, C.; Micoud, C.; Mir, L. M.; Belehradek, J., Jr.; Garrigos, M. Effects of detergents on P-glycoprotein atpase activity: differences in perturbations of basal and verapamil-dependent activities. *Cancer Biochem. Biophys.* **1998**, *16* (1−2), 85–110.
(23) Batrakova, E. V.; Li, S.; Li, Y.; Alakhov, V. Y.; Kabanov, A. V. Effect of pluronic P85 on ATPase activity of drug efflux transporters. *Pharm. Res.* **2004**, *21* (12), 2226–2233.

copolymers, in particular Pluronic P85, to a double punch effect of P-gp ATPase inhibition and intracellular ATP depletion, mediated via an alteration in mitochondrial membrane fluidity and membrane potential.[24] So far, it is unknown if TPGS 1000 exerts a similar effect on intracellular ATP levels and mitochondrial function.

Investigating P-gp conformational changes in the presence of TPGS 1000 with a UIC2 shift assay, and by studying the effects of TPGS 1000 on intracellular ATP levels, the present study aims to further elucidate the inhibitory mechanism of TPGS 1000 and its analogues on P-gp. Furthermore, the influence of time and side of access of TPGS 1000 to the efflux pump on its P-gp inhibitory activity was studied.

2. Materials and Methods

2.1. Materials. Minimum essential medium (MEM), Dulbecco's modified Eagle medium (DMEM), nonessential amino acids (NEAAs), and heat-inactivated fetal bovine serum (FBS) were purchased from GIBCO (Invitrogen GmbH; Karlsruhe, Germany). Monoclonal CD243 P-gp antibody clone UIC2 was obtained from Immunotech (Marseille, France). Alexa Fluor 488 conjugated antimouse Immunoglobulin G was acquired from Molecular Probes (Leiden, Netherlands). ^{3}[H]-Digoxin (40 Ci/mmol) was purchased from Perkin-Elmer (Rodgau, Germany). ATP assay mix and ATP standard, Bicinchonic Acid Kit, (*R*)-(+)-verapamil (Ver), cyclosporine A (CsA), sodium orthovanadate, Rhodamine 123 (RHO), digoxin (DIG), cholesterol, α- and γ-tocopherol, all polyethylene glycols, and all other materials were purchased from Sigma-Aldrich (Taufkirchen, Germany). Materials were stored as suggested by their manufacturer.

2.2. Synthesis and Purification of TPGS Analogues. TPGS 1000 and all analogues were synthesized according to the general synthetic procedure previously described.[16] Crude products were purified via preparative HPLC (Dynamax Microsorb C8, 250 × 41.4 mm i.d., 8 μm particles, 60 Å pore) using mobile phases (A, 25/75 methanol/acetonitrile (ACN); B, 25/75 isopropyl alcohol (IPA)/ACN; and C, IPA) with general gradient conditions of A for 24 min, B for 6 min and C for 12 min at a flow rate of ∼80 mL/min. The degree of purification was estimated by HPLC.

2.3. Cell Culture. Caco-2 cells, clone C2BBe1, were purchased from American Type Culture Collection (ATCC; Manassas, VA) and used at passage 70−92. They were kept at ∼37 °C in a controlled atmosphere of ∼5% CO_2 and a relative humidity of ∼85% with culture medium consisting of DMEM supplemented with 10% FBS and 1% NEAAs. For transport and UIC2 shift assay experiments, Caco-2 cells were grown for 21 to 25 days on #3460 polycarbonate membrane inserts (pore size 0.4 μm, 1.13 cm^2; Corning Inc. Life Sciences, Acton, MA) at a seeding density of ∼60,000 cells/cm^2. To ensure integrity of cell monolayers, transepithelial electrical resistance (TEER) was measured with a hand-held REMS electrical volt-ohm meter EVOM (World Precision Instruments; Sarasota, FL). Monolayers with a TEER ≥ 350 Ω·cm^2, with background subtracted, were used.

2.4. UIC2 Shift Assay. For the UIC2 shift assay experiments, Transwell grown Caco-2 cells were harvested after 21 days by trypsinization, washed and resuspended in Krebs Ringer Buffer (KRB: 14.0 mM NaCl, 0.3 mM KCl, 1.0 mM HEPES, 0.4 mM glucose, 0.14 mM $CaCl_2$, 0.25 mM $MgCl_2$, 0.15 mM K_2HPO_4) pH 7.4 supplemented with 1% BSA. Viable cells (0.5×10^6) in a total volume of 400 μL of KRB + 1% BSA were incubated (30 min; 37 °C) with primary monoclonal UIC2 antibody (5.0 μg). Whenever mentioned, prior to antibody addition, cells were preincubated (15 min; 37 °C) with CsA (5.0 μM), activated sodium orthovanadate (1.0 mM), Ver (50.0 μM), or TPGS 1000 (33.0 μM; 1.0 h of preincubation). UIC2 antibody was removed by washing the cells twice with KRB (5 mL) and resuspending in KRB + 1% BSA containing Alexa Fluor488 conjugated antimouse immunoglobulin G. After incubation (30 min; 37 °C), the secondary antibody was removed by washing twice with PBS (5 mL). Cells were resuspended in ice cold (4 °C) PBS (NaCl, 129 mM; KCl, 2.5 mM; Na_2HPO_4, 7.4 mM; KH_2PO_4, 1.3 mM) and analyzed with a BD FACS Calibur fluorescence-assisted cell sorter (BD Biosciences, Heidelberg, Germany). The fluorescence intensity associated with cells was expressed in fluorescence units (FU) on a log scale.

2.5. ATP Assay. For the ATP assay, Caco-2 cells were seeded on flat-bottom 96 well plates (∼20,000 cells/well) and grown to confluency for 10 days. On the day of the experiment, cells were pretreated with assay buffer (KRB + 10 mM glucose) for 30 min and then treated with vitamin E TPGS or analogue solutions (33.0 μM in KRB + 10 mM glucose) for 60 min. Following treatment, cells were washed twice with PBS (200 μL per well), solubilized in Triton X-100 (1.0%), and immediately frozen for subsequent ATP quantification (conducted within 24 h). ATP was determined using a luciferin/luciferase assay. For this purpose, cell lysate aliquots (100 μL) were mixed with ATP assay mix (100 μL). Light emission was measured with a Wallac 1450 Microbeta Luminescence counter (PerkinElmer, Rodgau, Germany). Raw data were collected as relative light units integrated over 20 s for samples and converted to ATP concentrations with the aid of a standard calibration curve obtained via ATP standards. ATP levels were normalized for protein content, determined via the Bicinchonic Acid Kit according to manufacturer's instructions.

2.6. Transport Assay. Drug transport was assessed in absorptive (apical to basolateral, Ap → Bl) and secretory (basolateral to apical, Bl → Ap) directions. Unless otherwise denoted, prior to the transport experiments, the monolayers were preincubated for 1.0 h in KRB pH 7.4. When varying the preincubation protocol, TPGS 1000 (33.0 μM) was present in the preincubation buffer for different durations as indicated in the text. Subsequently, at $t = 0$ min, a solution

(24) Batrakova, E. V.; Li, S.; Vinogradov, S. V.; Alakhov, V. Y.; Miller, D. W.; Kabanov, A. V. Mechanism of pluronic effect on P-glycoprotein efflux system in blood-brain barrier: Contributions of energy depletion and membrane fluidization. *J. Pharmacol. Exp. Ther.* **2001**, *299* (2), 483–493.

of RHO (13.0 μM) in KRB pH 7.4 or DIG (1.0 μM) in KRB pH 7.4 spiked with 0.1 nM ^{3}[H]-DIG was added to the donor compartment and pure KRB (pH 7.4 for both apical and basolateral side) was added to the receiver compartment. In the DIG experiments, the receiver solution consisted of 1% BSA in KRB (pH 7.4). In some experiments, the respective solutions on both sides contained TPGS 1000 (33.0 μM) while other experiments had TPGS 1000 present on the receiver or donor side only.

Monolayers were agitated using an orbital shaker (IKA-Werke GmbH & CO KG; Staufen, Germany) at 100 ± 20 rpm. Samples (200 μL) were collected from the receiver compartment at regular time points for up to 300 min. After each sampling, an equal volume of fresh transport buffer (~37 °C) was added to the receiver compartment. RHO was quantified using a Cytofluor-2 fluorescence plate reader (Perkin-Elmer Biosystems; Weiterstadt, Germany) operating at excitation wavelength of 485 nm with an emission wavelength of 530 nm. DIG was quantified via radioactivity measurements using Tri-Carb 2100TR liquid scintillation analyzer (Packard BioScience, Meriden, CT) after the addition of 2.0 mL of scintillation fluid (UltimaGold; Perkin-Elmer, Rodgau, Germany).

2.7. Apparent Permeability. Flux was determined using receiver compartment RHO steady-state appearance rates ($\Delta Q/\Delta t$). P_{app} across Caco-2 monolayers was calculated via

$$P_{app} = \frac{\Delta Q}{\Delta t \cdot A \cdot C_0}$$

P_{app} is apparent permeability coefficient [cm/s], $\Delta Q/\Delta t$ is permeability rate [μg/s], C_0 is initial concentration in donor chamber [μg/cm^3], and A is membrane surface area [cm^2].

2.8. Statistical Analysis. Results are expressed as mean ± SD or mean ± SEM. Significance of difference was determined by one-way analysis of variances (ANOVA) followed by Neumann−Keuls−Student or Holm−Sidak posthoc tests.

3. Results

3.1. UIC2 Shift Assay. UIC2 reactivity shift assay was used to study P-gp conformational transitions in the presence of TPGS 1000. The known P-gp substrates, and competitive inhibitors, cyclosporine A (CsA) and verapamil (Ver) were included as reference compounds. Sodium orthovanadate, which traps the efflux pump in a transition state, was also used. Fluorescence intensity was quantified using a fluorescence activated cell sorter. Indicating increased UIC2 reactivity with its epitope in P-gp, both CsA (10.0 μM) and Ver (50.0 μM) shifted intensity of the fluorescence to higher levels (Figure 1). The shift was stronger for CsA, which raised the mean fluorescence intensity (F_{mean}) from 21.8 ± 4.3 FU in the control to 106.2 ± 9.2 FU; whereas Ver only increased F_{mean} to a level of 45.4 ± 4.7 FU. In contrast, both activated sodium orthovanadate (1.0 mM) and TPGS 1000 (33.0 μM) induced a reduction in UIC2 binding with the effect being more pronounced for orthovanadate (F_{mean} = 4.0 ± 1.3 FU) than for TPGS 1000 (F_{mean} = 18.6 ± 3.9 FU).

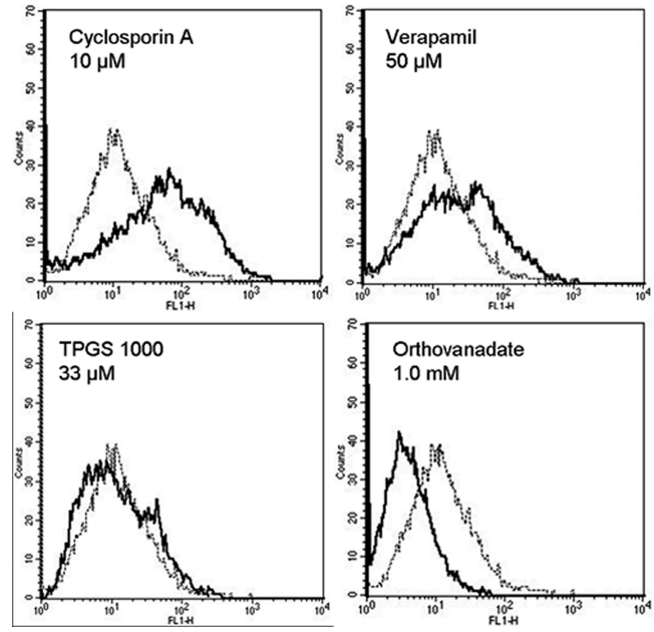

Figure 1. Monoclonal antibody UIC2 reactivity with P-gp in Caco-2 cells. Caco-2 cells were incubated with UIC2 antibody in the absence (dotted lines) and presence of P-gp substrates/modulators (solid lines); 10.0 μM cyclosporine A, 50.0 μM verapamil, 33.0 μM TPGS 1000, 1.0 mM orthovanadate.

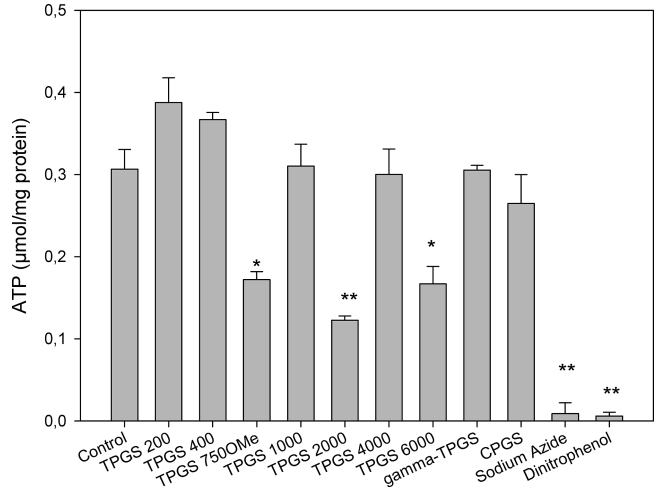

Figure 2. Intracellular ATP levels in Caco-2 cells after incubation with different TPGS analogues (33.0 μM) for 60 min; mean ± SEM, n = 12; * = significantly different from untreated control. ($P < 0.05$)

3.2. ATP Assay. Studying surfactant effect on intracellular ATP (Figure 2), compared to control (0.31 ± 0.08 μmol/mg protein), TPGS 1000 at a concentration of 33.0 μM (0.32 ± 0.09 μmol/mg protein) did not statistically alter (P = 0.647) intracellular ATP concentrations in Caco-2 cells after incubating (60 min). When other TPGS 1000 concentrations were evaluated, no dose response relationship was observed;

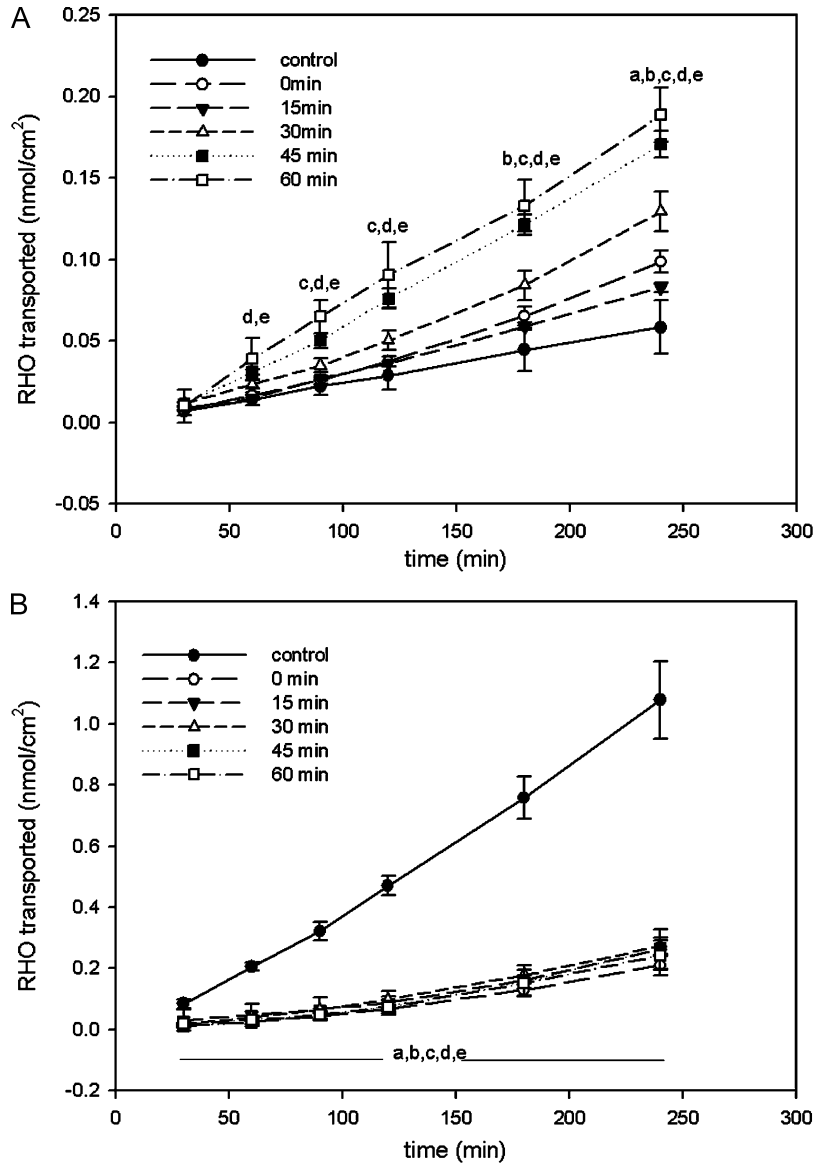

Figure 3. (A) Rhodamine 123 (13.0 μM) time-course transport across Caco-2 monolayers in the presence of TPGS 1000 (33.0 μM) on both the apical and basolateral sides using different preincubation times; absorptive transport, mean $\pm$ SD, $n = 12$; inset shows key for control group and 0, 15, 30, 45, and 60 min preincubation groups; a−e indicates treatment group is significantly different from untreated control ($P < 0.05$). (B) Rhodamine 123 (13.0 μM) time-course transport across Caco-2 monolayers in the presence of TPGS 1000 (33.0 μM) on both the apical and basolateral sides using different preincubation times; secretory transport, mean $\pm$ SD, $n = 12$; inset shows key for control group and 0, 15, 30, 45, and 60 min preincubation groups; a−e indicates treatment group is significantly different from untreated control ($P < 0.05$).

all results varied around control values, with no statistically significant effects ($P < 0.05$) detectable even at very high TPGS 1000 concentrations up to 3.3 mM (data not shown).

In a head to head comparison of different P-gp active and nonactive TPGS analogues (Figure 2), reduced ATP levels ($P < 0.05$) were observed in the presence of TPGS 750-OMe, TPGS 6000, and TPGS 2000, the latter presenting the strongest effect. However, intracellular ATP level reduction in all three cases fell short to the total ATP depletion observed via metabolic inhibitors sodium azide or dinitrophenol, resulting in ATP levels of 0.01 $\pm$ 0.05 μmol/mg protein and 0.01 $\pm$ 0.02 μmol/mg protein, respectively ($P <$ 0.01). A noneffect was observed with other TPGS analogues (TPGS 200, TPGS 400, TPGS 4000, gamma TPGS 1000 and the cholesterol analogue CPGS 1000).

3.3. Influence of Time and Side of Access. Preincubation conditions and application side were varied to determine the influence of various experimental parameters on the degree of inhibition; the results provide additional data to elucidate the inhibitory mechanism. As presented in Figure 3A,B, bidirectional RHO transport was investigated using different preincubation times (0, 15, 30, 45, and 60 min) in the presence of TPGS

Table 1. Apparent Permeability and Efflux Ratios of Rhodamine 123 (13.0 μM) Transport across Caco-2 Monolayers in the Presence of TPGS 1000 (33.0 μM) on Both the Apical and Basolateral Sides Using Different Preincubation Times[a]

	$P_{app} \times 10^{-6}$ cm/s ± SD		
experiment	Ap → Bl	Bl → Ap	efflux ratio (ER) ± SD
control	0.25 ± 0.07	4.52 ± 0.47	18.4 ± 6.9
0 min preincubation	0.41 ± 0.03*	1.17 ± 0.09**	2.8 ± 0.4*
15 min preincubation	0.55 ± 0.02**	1.11 ± 0.30**	2.0 ± 0.7**
30 min preincubation	0.65 ± 0.05**	1.10 ± 0.10**	1.8 ± 0.3**
45 min preincubation	0.81 ± 0.02**	1.05 ± 0.12**	1.3 ± 0.2**
60 min preincubation	0.86 ± 0.12**	0.99 ± 0.11**	1.1 ± 0.4**

[a] Mean ± SD, $n = 12$; * = significantly different from untreated control ($P < 0.05$), ** = significantly very different from untreated control ($P < 0.01$).

1000. Absorptive RHO transport increase in the presence of TPGS 1000 was clearly time dependent; the shorter the preincubation time, the longer the delay in the onset of action (Figure 3A). As a result, if Caco-2 cell monolayers were preincubated for only 0, 15, or 30 min with TPGS 1000, the increase in absorptive permeability at the end of the experiment was weaker; statistically different ($P < 0.05$) RHO levels were only observed after 90 to 240 min, and transport rates kept increasing until very late into the experiment. Consequently, constant flux was not reached and determination of meaningful P_{app} values becomes nearly impossible for these treatment groups. Nonetheless, if one averages flux over the entire experiment, averaged P_{app} values reveal statistical differences in absorptive transport rates compared to control for all TPGS 1000 preincubation times (Table 1). However, the calculated P_{app} value after 60 min of preincubation ($0.86 \pm 0.12 \times 10^{-6}$ cm/s) was about twice as high as the absorptive P_{app} value for 0 min preincubation time ($0.41 \pm 0.03 \times 10^{-6}$ cm/s). The 45 min preincubation time profile and P_{app} value do not differ significantly from the 60 min preincubation values. Statistically different RHO levels were observed 30−60 min into the experiment. In the case of secretory RHO transport, regardless of the length of preincubation time (Figure 3B), TPGS 1000 had a large and immediately noteworthy effect relative to control with a slightly more pronounced reduction of P_{app} values with longer preincubation (Table 1).

In addition to RHO, digoxin (DIG)—another well-known P-gp substrate—transport with varying times of TPGS 1000 preincubation was investigated. Compared to control, a strong increase in absorptive DIG transport was noticeable for all TPGS 1000 treated experiments with no discernible differences between cell monolayers preincubated with TPGS 1000 (Figure 4A). For these treatment groups, absorptive transport increase was already statistically significant ($P < 0.05$) at the first sampling point (30 min) after substrate addition. Monolayers not preincubated with TPGS 1000 showed a delayed DIG transport increase which became statistically significant ~60 min into the experiment. DIG flux via non-preincubated cells eventually caught up with the TPGS 1000 preincubated groups; the overall amount of DIG transported remained significantly lower than in the preincubated cells. Similar to the RHO experiments, all TPGS 1000 treated cell monolayers had a significantly lower secretory DIG transport (Figure 4B); no TPGS 1000 time-dependent preincubation DIG transport reduction was observed.

After probing time-dependent preincubation, we investigated the impact of inhibitor application side on absorptive and secretory RHO transport without preincubation. We placed TPGS 1000 on the apical side only, basolateral side only, and both sides (Figure 5A,B). Independent of application side, it took 150−210 min to observe a statistically significant enhancement in absorptive RHO transport rate. The effect was slightly delayed when TPGS 1000 was only placed on the basolateral side and also afforded lower, but not significantly different, permeability values after 300 min: $0.33 \pm 0.04 \times 10^{-6}$ cm/s for the basolateral treatment group compared to $0.37 \pm 0.04 \times 10^{-6}$ cm/s for the apical treatment group (Figure 5A, Table 2). The impact of TPGS 1000 on secretory RHO transport was instantaneous (Figure 5B) and showed the same time-dependent behavior as absorptive RHO transport. When TPGS 1000 was only placed on the basolateral side, significantly weaker effects on RHO efflux ($P_{app} = 1.31 \pm 0.14 \times 10^{-6}$ cm/s) were observed, while no differences could be found between applications on both sides ($P_{app} = 0.84 \pm 0.17 \times 10^{-6}$ cm/s) versus apical side only ($P_{app} = 0.91 \pm 0.15 \times 10^{-6}$ cm/s, Table 2).

4. Discussion

Previous work conducted in our laboratories established the notion that TPGS 1000 (D-α-tocopheryl polyethylene glycol 1000 succinate), a nonionic surfactant, modulates P-glycoprotein (P-gp) efflux transport via P-gp ATPase inhibition.[21] However, it remained unclear if the ATPase inhibition was due to a direct interaction with P-gp NBDs, an allosteric modulation of the efflux transporter via one of the nontransport active binding sites, steric blocking of substrate binding in the membrane, or a combination thereof. To further investigate these possible mechanisms of TPGS 1000 interaction with P-gp, conformational changes in the efflux pump in the presence of TPGS 1000 were investigated using the UIC2 shift assay. A monoclonal antibody, UIC2 recognizes human P-gp on the cell surface and strongly inhibits P-gp mediated drug efflux.[25] In contrast to similar P-gp antibodies, UIC2 reactivity has P-gp functional state sensitivity. UIC2 binding to P-gp becomes increased upon substrate binding, in cells whose ATP levels are depleted, or whose nucleotide binding sites are inactivated via mutation.[26] On the other hand, UIC2 binding decreases in the presence of vanadate, which traps P-gp in a transition state

(25) Mechetner, E.; Roninson, I. Efficient Inhibition of P-Glycoprotein-Mediated Multidrug Resistance with a Monoclonal Antibody. *Proc. Natl. Acad. Sci. U.S.A.* **1992**, *89* (13), 5824–5828.

(26) Mechetner, E. B.; Schott, B.; Morse, B. S.; Stein, W. D.; Druley, T.; Davis, K. A.; Tsuruo, T.; Roninson, I. B. P-glycoprotein function involves conformational transitions detectable by differential immunoreactivity. *Proc. Natl. Acad. Sci. U.S.A.* **1997**, *94* (24), 12908–12913.

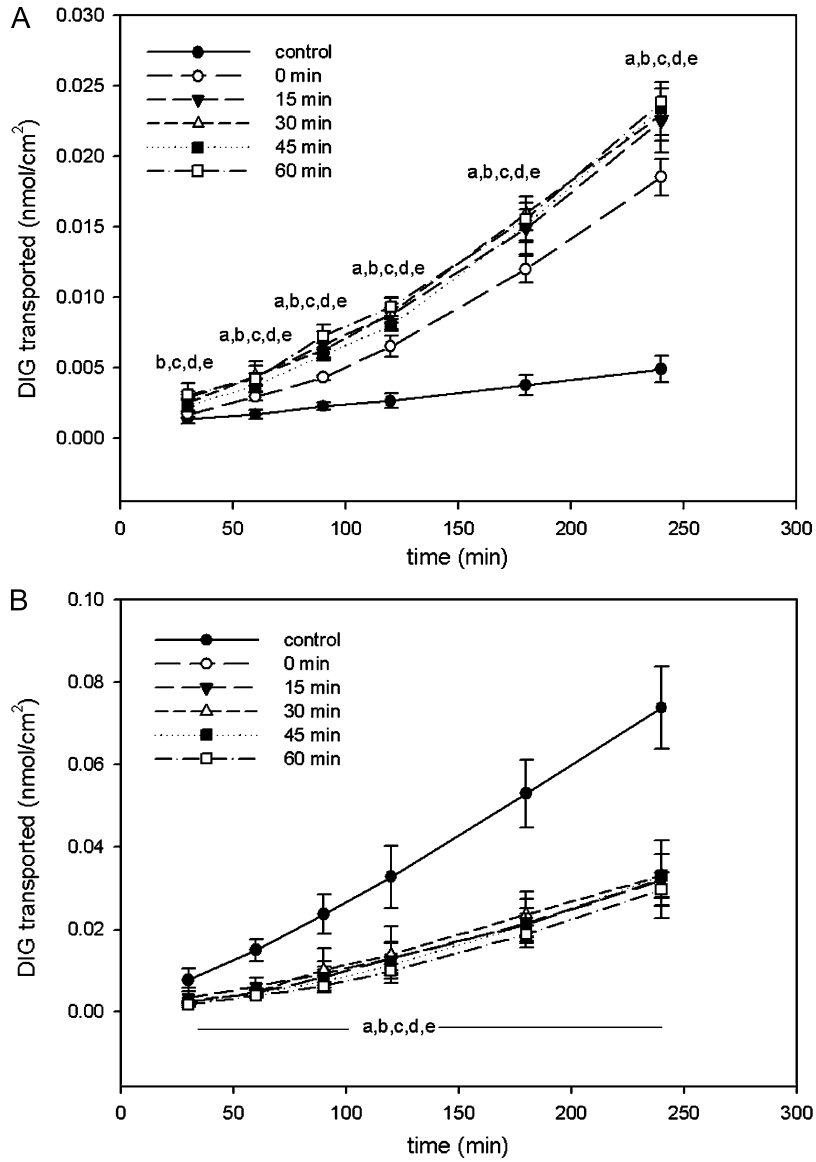

Figure 4. (A) Digoxin (1.0 μM) time-course transport across Caco-2 monolayers in the presence of TPGS 1000 (33.0 μM) on both the apical and basolateral sides using different preincubation times; absorptive transport, mean ± SD, $n = 4-6$; inset shows key for control group and 0, 15, 30, 45, and 60 min preincubation groups; a−e indicates treatment group is significantly different from untreated control ($P < 0.05$). (B) Digoxin (1.0 μM) time-course transport across Caco-2 monolayers in the presence of TPGS 1000 (33.0 μM) on both the apical and basolateral sides using different preincubation times; secretory transport, mean ± SD, $n = 4-6$; inset shows key for control group and 0, 15, 30, 45, and 60 min preincubation groups; a−e indicates treatment group is significantly different from untreated control ($P < 0.05$).

by forming an irreversible ternary complex with ADP and P-gp.[27,28] The differences in UIC2 reactivity are ascribed to differing numbers of P-gp molecules presenting the epitope recognized by UIC2 at the cell surface, thus reflecting P-gp conformational changes during its catalytic cycle. Residues in the extracellular loop between TM5 and TM6 are directly involved in the UIC2 epitope.[29] TM6 has been shown to be actively involved in the drug transport process, and the proximity of this region to TM6 may help explain why UIC2 binding has high functional state sensitivity and why UIC2 binding inhibits P-gp mediated drug transport. As previously

(27) Urbatsch, I. L.; Sankaran, B.; Weber, J.; Senior, A. E. P-glycoprotein Is Stably Inhibited by Vanadate-induced Trapping of Nucleotide at a Single Catalytic Site. *J. Biol. Chem.* **1995**, *270* (33), 19383–19390.

(28) Druley, T. E.; Stein, W. D.; Roninson, I. B. Analysis of MDR1 P-Glycoprotein Conformational Changes in Permeabilized Cells Using Differential Immunoreactivity. *Biochemistry* **2001**, *40* (14), 4312–4322.

(29) Zhou, Y.; Gottesman, M. M.; Pastan, I. The extracellular loop between TM5 and TM6 of P-glycoprotein is required for reactivity with monoclonal antibody UIC2. *Arch. Biochem. Biophys.* **1999**, *367* (1), 74–80.

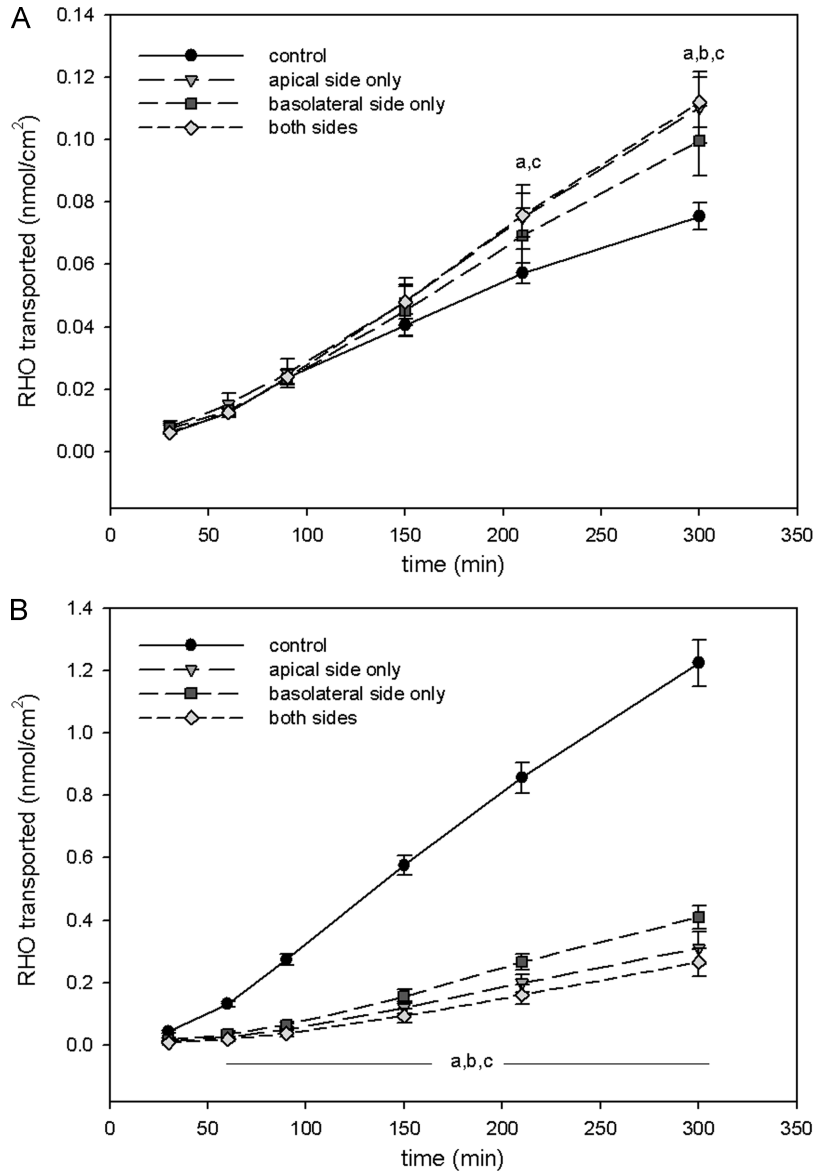

Figure 5. (A) Rhodamine 123 (13.0 μM) time-course transport across Caco-2 monolayers in the presence of TPGS 1000 (33.0 μM) on apical, basolateral, or both sides with preincubation without TPGS 1000; absorptive transport, mean $\pm$ SD, $n = 3-6$; inset shows key for control, application on apical side, application on basolateral side, and application on both sides; a−c indicates treatment group is significantly different from untreated control ($P < 0.05$). (B) Rhodamine 123 (13.0 μM) time-course transport across Caco-2 monolayers in the presence of TPGS 1000 (33.0 μM) on apical, basolateral, or both sides with preincubation without TPGS 1000; secretory transport, mean $\pm$ SD, $n = 3-6$; inset shows key for control, application on apical side, application on basolateral side, and application on both sides; a−c indicates treatment group is significantly different from untreated control ($P < 0.05$).

described,[26] known P-gp substrates and competitive inhibitors, CsA and Ver, significantly increased reactivity of UIC2 with P-gp in Caco-2 cells (Figure 1). In contrast, TPGS 1000 slightly shifted UIC2 binding to lower levels; it was not statistically significant. Hence, these results support the notion that TPGS 1000 does not bind to one of P-gp's transport active drug binding sites, either as a substrate or as a competitive inhibitor. UIC2 binding in TPGS 1000 treated Caco-2 cells was only slightly reduced, distinguishing it from orthovanadate which significantly lowers UIC2 binding. Orthovanadate forms a ternary complex with ADP and the P-gp NBD,[27] inhibiting nucleotide dissociation and reducing the number of UIC2-recognizable P-gp molecules. Therefore, trapping P-gp in a transition state via TPGS 1000 intracellular complex formation seems unlikely. The almost noneffect of TPGS 1000 on UIC2 binding also provides evidence against an allosteric modulation of P-gp targeting the Cis(Z)-flupentixol binding site. Cis(Z)-flupentixol, a P-gp allosteric inhibitor, has been demonstrated to reduce UIC2 reactivity with P-gp by blocking substrate translocation and dissociation.[30]

Furthermore, intracellular ATP depletion by TPGS 1000 may be excluded; a result which should produce a noticeable increase of UIC2 recognizable molecules.[26] Intracellular ATP

Table 2. Apparent Permeability and Efflux Ratios of Rhodamine 123 (13.0 μM) Transport across Caco-2 Monolayers in the Presence of TPGS 1000 (33.0 μM) on Apical, Basolateral, or Both Sides with Preincubation without TPGS 1000[a]

	$P_{app} \times 10^{-6}$ cm/s ± SD		
experiment	Ap → Bl	Bl → Ap	efflux ratio (ER) ± SD
control	0.28 ± 0.02	4.25 ± 0.33	15.3 ± 2.1
apical side only	0.37 ± 0.04*	0.91 ± 0.15**	2.4 ± 0.7**
basolateral side only	0.33 ± 0.04*	1.31 ± 0.14*	3.8 ± 0.8*
both sides	0.38 ± 0.04*	0.84 ± 0.17**	2.2 ± 0.6**

[a] Mean ± SD, n = 3−6; * = significantly different from untreated control ($P < 0.05$), ** = significantly very different from untreated control ($P < 0.01$).

depletion was previously proposed as a mechanism of action for Pluronic P85, another nonionic surfactant known to inhibit P-gp and P-gp ATPase.[31,32] In contrast, TPGS 1000 shows similarity to polyoxyethylene (40) stearate, a material known to effect P-gp ATPase while not influencing intracellular ATP or mitochondrial function.[33] As a result, there does not appear to be a common inhibitory mechanism for all nonionic surfactants; the interaction with P-gp needs to be individually investigated for each surfactant until a broader structure inhibition relationship becomes elucidated.

In agreement with findings in the UIC2 shift assay, TPGS 1000 (33.0 μM) showed no significant effect in the ATP assay; TPGS 1000 neither reduced nor increased intracellular ATP levels, independent of the concentrations employed (data not shown). A reduction of intracellular ATP was observed in the presence of TPGS analogues TPGS 750-OMe, TPGS 2000 and TPGS 6000 although their effect fell well short of total ATP depletion as observed in the presence of metabolic inhibitor cocktails sodium azide (10.0 mM)/2-desoxyglucose and 2,4-dinitrophenol (1.0 mM)/2-deoxyglucose. No correlation between the effect of TPGS analogues on intracellular ATP levels and their previously investigated P-gp inhibitory properties could be found.[16,21,34] In particular, no correlation regarding TPGS analogue inhibitory effect on P-gp ATPase, one of the central steps in the inhibition mechanism, was observed.[21] Some TPGS analogues with strong P-gp modulating and P-gp ATPase inhibiting effects, similarly to TPGS 1000, such as γ-TPGS or the cholesterol derivative (CPGS) did not alter ATP levels; whereas non- or only weak P-gp active analogues (e.g., TPGS 6000) lowered intracellular ATP content (Figure 3). Therefore, it seems more likely that the reduced ATP levels observed for some analogues are not due to a systematic effect on mitochondrial membranes and function, as observed for the Pluronics, but rather unspecific cytotoxic disturbances not readily detected in previously conducted lactate dehydrogenase (LDH) leakage, an assay which reflects membrane destabilization.[16]

Interestingly, while varying preincubation conditions, secretory transport was less impacted by changes in the experimental protocol than absorptive transport; secretory transport decrease was instantaneous for the two investigated P-gp substrates RHO and DIG (Figures 3B and 4B), while RHO absorptive transport varied greatly between different preincubation times in the presence of TPGS 1000. A possible effect of TPGS 1000, or its analogues, on tight junctional integrity and function may be ruled out as a possible explanation for the differences between the two RHO transport directions. Transport of sodium fluorescein, a paracellularly transported non-P-gp substrate, was unaffected by the presence of TPGS 1000 (33.0 μM) in either transport direction affording low P_{app} values and an efflux ratio of 1.12 and 1.24 in the absence and presence of TPGS 1000, respectively (data not shown). Instead, the distinct transport paths as previously described by Troutman and Thakker may explain the discriminative effect of TPGS 1000 on RHO transport;[35] they denote that absorptive RHO transport becomes limited via the paracellular route, while secretory transport mainly occurs via a basolaterally located uptake transporter with subsequent P-gp mediated efflux at the apical interface. In consequence, RHO absorptive transport requires a longer time period (during which RHO enters the cells via the "backdoor") before P-gp becomes exposed to significant amounts of RHO; thereby time-dependent efflux and inhibition activity are observed in RHO *in vitro* experiments. In the case of secretory RHO transport, this exposure occurs much faster and the effects on P-gp activity become immediately apparent. This hypothesis may be supported by the absorptive and secretory DIG transport results, where TPGS 1000 P-gp inhibitory effects were instantaneous for all preincubated Caco-2 cells and independent of preincubation time. Full inhibitory effects are only delayed when TPGS 1000 and the substrate (DIG) are simultaneously applied (0 min preincubation). However the extent of the effect was much weaker compared to RHO absorptive transport. DIG may be considered as a "pure P-gp substrate", which gets transported via the transcellular route

(30) Maki, N.; Hafkemeyer, P.; Dey, S. Allosteric modulation of human P-glycoprotein. Inhibition of transport by preventing substrate translocation and dissociation. *J. Biol. Chem.* **2003**, *278* (20), 18132–18139.

(31) Rapoport, N.; Marin, A. P.; Timoshin, A. A. Effect of a Polymeric Surfactant on Electron Transport in HL-60 Cells. *Arch. Biochem. Biophys.* **2000**, *384* (1), 100–108.

(32) Batrakova, E. V.; Li, S.; Elmquist, W. F.; Miller, D. W.; Alakhov, V. Y.; Kabanov, A. V. Mechanism of sensitization of MDR cancer cells by Pluronic block copolymers: Selective energy depletion. *Br. J. Cancer* **2001**, *85* (12), 1987–1997.

(33) Zhu, S.; Huang, R.; Hong, M.; Jiang, Y.; Hu, Z.; Liu, C.; Pei, Y. Effects of polyoxyethylene (40) stearate on the activity of P-glycoprotein and cytochrome P450. *Eur. J. Pharm. Sci.* **2009**, *37* (5), 573–580.

(34) Wempe, M. F.; Wright, C.; Little, J. L.; Lightner, J. W.; Large, S. E.; Caflisch, G. B.; Buchanan, C. M.; Rice, P. J.; Wacher, V. J.; Ruble, K. M.; Edgar, K. J. Inhibiting efflux with novel non-ionic surfactants: Rational design based on vitamin E TPGS. *Int. J. Pharm.* **2009**, *370* (1−2), 93–102.

(35) Troutman, M. D.; Thakker, D. R. Rhodamine 123 requires carrier-mediated influx for its activity as a P-glycoprotein substrate in Caco-2 cells. *Pharm. Res.* **2003**, *20* (8), 1192–1199.

in both transport directions and thus directly subjected to P-gp efflux in both cases.[39] Therefore, TPGS 1000s P-gp inhibitory potential appears to be the same in both transport directions. However, atypical P-gp substrates (e.g., RHO) afford an amplified TPGS 1000 preincubation time and transport direction dependent effect.

A similar variation in sensitivity to changes in the protocol with transport directions was observed when TPGS 1000 application side was altered (Figure 5AB). Independent of side of application, TPGS 1000 influenced absorptive as well as secretory RHO transport, although the effect was slightly weaker in both transport directions when the surfactant was placed only in the basolateral compartment. As in the previous experiments with no preincubation, it took up to 1.5−2.0 h to observe an effect on RHO absorptive transport. In addition, the effect was further delayed when TPGS 1000 was only added to the basolateral side, indicating that TPGS 1000 must first traverse the cell monolayer to reach its site of action in the apical cell membrane and inhibit P-gp mediated efflux. Consequently, P-gp inhibition by TPGS 1000 seems to be the result of a direct interaction with the efflux pump rather than indirect effects translated through the cell membrane, results previously demonstrated via electron spin resonance (ESR) studies illustrating no significant changes in the P-gp membrane environment in the presence of TPGS 1000.[21] The strong influence of preincubation conditions, and side of access to the efflux transport, may also help explain contradictory literature reports on TPGS 1000s inhibitory potency. Some groups have observed strong inhibitory influence in both transport directions,[14,36−38] while others have reported no effect on absorptive transport, or even a reduction of absorptive transport relative to control.[20,39] Thus, P-gp substrate choice and protocol, in particular TPGS 1000 preincubation time, appears to explain the contradictory findings. In our RHO experiments, merely looking at absorptive transport rates without preincubation would significantly underestimate TPGS 1000 inhibitory potency, while sufficient preincubation times and/or bidirectional studies taking into account efflux ratios (ER, Tables 1 and 2) help to illustrate the extent of P-gp inhibition. This further stresses the importance of investigating and optimizing experimental protocol with regard to preincubation and choice of model substrate in evaluating novel P-gp modulators.

5. Conclusion

TPGS 1000s *in vitro* P-gp inhibitory mechanism was further investigated. TPGS 1000 does not appear to be a P-gp substrate or a competitive inhibitor. Intracellular ATP depletion, which has been associated with the inhibitory effects of other surfactants on P-gp, was ruled out. The increased inhibitory effect of TPGS 1000 on unoccupied P-gp suggests an allosteric modulation not involving the Cis(Z)-flupentixol binding site.

Acknowledgment. We thank Katja Klein and Petra Koenig at Saarland University for their technical assistance with the Caco-2 cell culture. Judith Wollscheidt is thanked for her help with the ATP assay.

MP900191S

(36) Bogman, K.; Zysset, Y.; Degen, L.; Hopfgartner, G.; Gutmann, H.; Alsenz, J.; Drewe, J. P-glycoprotein and surfactants: effect on intestinal talinolol absorption. *Clin. Pharmacol. Ther.* **2005**, *77* (1), 24–32.

(37) Yu, L.; Bridgers, A.; Polli, J.; Vickers, A.; Long, S.; Roy, A.; Winnike, R.; Coffin, M. Vitamin E-TPGS increases absorption flux of an HIV protease inhibitor by enhancing its solubility and permeability. *Pharm. Res.* **1999**, *16* (12), 1812–1817.

(38) Varma, M. V.; Panchagnula, R. Enhanced oral paclitaxel absorption with vitamin E-TPGS: effect on solubility and permeability in vitro, in situ and in vivo. *Eur. J. Pharm. Sci.* **2005**, *25* (4−5), 445–453.

(39) Troutman, M.; Thakker, D. Efflux ratio cannot assess P-glycoprotein-mediated attenuation of absorptive transport: asymmetric effect of P-glycoprotein on absorptive and secretory transport across Caco-2 cell monolayers. *Pharm. Res.* **2003**, *20* (8), 1200–1209.